Journal of Thermal Analysis and Calorimetry, Vol. 85 (2006) 2, 309–314

PHASE EQUILIBRIA IN THE $Ag_4SSe–As_2Se_3$ SYSTEM

V. Vassilev[*], *L. Aljihmani and V. Parvanova*

University of Chemical Technology and Metallurgy, 8 Kliment Ohridski blvd., 1756 Sofia, Bulgaria

The phase diagram of the system $Ag_4SSe–As_2Se_3$ is studied by means of X-ray diffraction, differential thermal analyses and measurements of the microhardness and the density of the materials. The unit-cell parameters of the intermediate phases $3Ag_4SSe·As_2Se_3$ (phase A) and $Ag_4SSe·2As_2Se_3$ (phase B) are determined as follows for phase A: a=4.495 Å, b=3.990 Å, c=4.042 Å, α=89.05°, β=108.98°, γ=92.93°; for phase B: a=4.463 Å, b=4.136 Å, c=3.752 Å, α=118.60°, β=104.46°, γ=83.14°. The phase $3Ag_4SSe·As_2Se_3$ and $Ag_4SSe·2As_2Se_3$ have a polymorphic transition $\alpha\leftrightarrow\beta$ consequently at 105 and 120°C. The phase A melts incongruently at 390°C and phase B congruently at the same temperature.

Keywords: *$Ag_4SSe–As_2Se_3$, differential thermal analysis, phase diagram, X-ray diffraction*

Introduction

The combination of the compounds Ag_4SSe and As_2Se_3 has not been studied in relation with the phase equilibria. Investigation of such a binary system is of a definite scientific and practical interest because components with different properties are involved. The composition Ag_4SSe exists in the nature and is known as the mineral Aquilarite [1, 2]. It is synthesised for first time by Earley by means of a direct synthesis [3]. Its existence is confirmed also at investigation of the phase diagram of the system $Ag_2S–Ag_2Se$ [4]. The phase transition α-$Ag_4SSe\rightarrow\beta$-Ag_4SSe takes place at 100±5°C and the compound Ag_4SSe melts at 815°C [4]. The thermal energy gap of Ag_4SSe is 0.24±0.01 eV [5]. The conductivity of the material and its electron mobility and concentration at 300 K are 500 S cm^{-1}, 350 cm^2 V^{-1} s^{-1} and $6.5\cdot10^{18}$ cm^{-3} [5]. Ag_4SSe exhibits good thermoelectric properties [5, 6].

As_2Se_3 exists both in glassy and in crystal state. Under standard conditions of synthesis and quick cooling As_2Se_3 is obtained in the form of glass. On continuous heat treatment under $T>T_{cr}$ (T=const) and slow cooling As_2Se_3 is obtained in crystal state. As_2Se_3 is a high-ohm semiconductor. At T=300 K the crystal As_2Se_3 has electrical conductivity of the order of 10^{-13} S cm^{-1}, and the glassy 10^{-12} S cm^{-1}. The thermal energy gap is 1.84 and 1.90 eV, respectively [7]. As_2Se_3 crystallizes in a monoclinic lattice structure.

The main goal of this work is the investigation of the phase equilibria in the system $Ag_4SSe–As_2Se_3$ by means of the conventional differential thermal analysis (DTA) [8–11], and X-ray powder diffraction (XRD) [8, 9] as well as determining the limits of the solid solutions and the compositions of the intermediate phases (if such exist), thus building a base for a further complex investigation.

Experimental

The system $(Ag_4SSe)_{100-x}(As_2Se_3)_x$ was studied by the help of 17 compositions within the concentration range 0–100 mol% As_2Se_3. The compositions were prepared through a direct mono-temperature synthesis [7] mixing in proper ratio Ag_4SSe and As_2Se_3 in vacuumed and sealed quartz ampoules. Ag_4SSe and As_2Se_3 were obtained by the same method from initial elements with purity 4N (Ag, S) and 5N (As, Se). The maximum temperature and the duration of the synthesis were 900°C and 2 h. A vibrational stirring of the melt was applied. As a final step the melts were homogenized at 300°C for 1 h and frozen with water+ice.

The phase transformations in the samples were investigated by means of several methods as follows: derivatograph (equipment of the system Paulik–Paulik–Erdey made by MOM, Hungary) at a heating rate of 10°C min^{-1}; reference substance (calcinated γ-Al_2O_3) and the studied substance weighed ≈0.3 g and was placed in evacuated and sealed quartz Stepanov's ampoules at pressure equal to $\approx0.1\cdot10^{-2}$ Pa; XRD (equipment TUR-M61) with CuK_α irradiation and Ni-filter, θ=5–40°, measurements of the microhardness (instrument PMT-3 and microscope MIM-7 at loading 10 and 20 g) and of the density (hydrostatic technique with toluene as reference liquid).

---

[*] Author for correspondence: venciv@uctm.edu

1388–6150/$20.00

Akadémiai Kiadó, Budapest, Hungary
Springer, Dordrecht, The Netherlands

Results and discussion

The data obtained from the X-ray diffraction analyses are summarized in a schematic diagram (Fig. 1).

The schematic diagram of the X-ray diffraction lines of the starting components As_2Se_3 and Ag_4SSe is in a complete agreement with the results reported previously in the literature of Ag_4SSe [1] and As_2Se_3 [12].

Within the range of concentrations 0–100 mol% As_2Se_3 new lines are observed, different from those of Ag_4SSe and As_2Se_3. They are of maximum intensity and best pronounced for compositions containing 25.0 and 66.7 mol% As_2Se_3. These data suggest the existence of two intermediate phases with the most probable compositions $3Ag_4SSe{\cdot}As_2Se_3$ (phase A) and $Ag_4SSe{\cdot}2As_2Se_3$ (phase B).

The unit-cell parameters of phase A and phase B previously are determined by the Ito's method [13] as follows: for phase A: a=4.495 Å, b=3.990 Å, c=4.042 Å, α=89.05°, β=108.98°, γ=92.93°; for phase B: a=4.463 Å, b=4.136 Å, c=3.752 Å, α=118.60°, β=104.46°, γ=83.14°.

The indexing data of these phases are given in Tables 1 and 2, respectively.

We determined the temperatures of the different phase transitions by the heating curves (the samples were tempered in advance throughout 30 h at T=300±10°C). The results are summarized in Table 3.

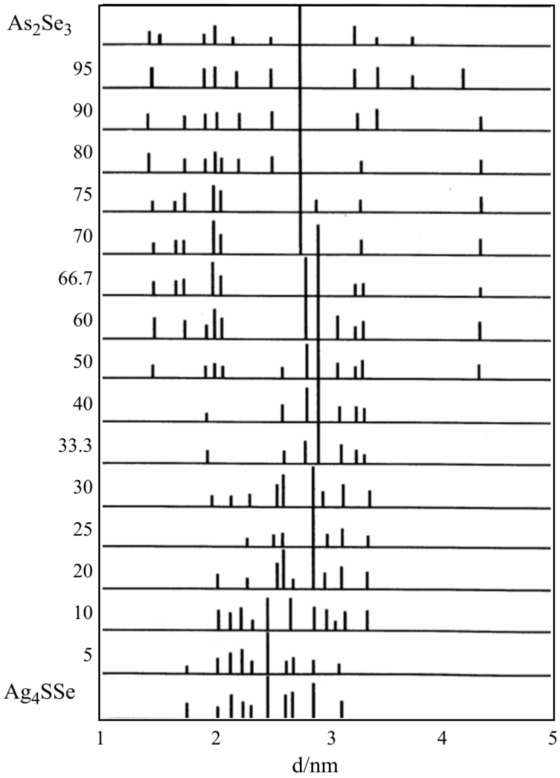

Fig. 1 Schematic diagram of the X-ray diffraction lines for the system Ag_4SSe–As_2Se_3

The thermal effects of the samples rich of As_2Se_3 were not well marked because of the characteristic of the compound As_2Se_3 (difficult to crystallize). Many authors studying binary systems, one of the components of which is As_2Se_3, have run into such difficulties [14].

The observed effects of the thermograms are endothermal. The effects of column 9 of Table 3 are marked best (sharp pick and large area) and they correspond to the liquidus line.

There are several groups of endothermal effects the temperature of which does not depend on the composition of the samples, and these are the thermal effects of columns 1 and 3 to 7 inclusive. The temperature of the effects of columns 2 and 8 depend on the composition and most logically they belong to the solidus line. The area of the thermal effects with 390°C (column 7) and the effects of the liquidus line from 60 to 80 mol% As_2Se_3 depend on the composition of the samples as the maximum area is of samples containing 25.0 and 66.7 mol% As_2Se_3, respectively. Such dependency is characteristic either of chemical compound formation or of a non-variant point. Dependency is also observed in the thermal effects of columns 3 and 4 between the area and the composition with maximum area of samples containing 25.0 and 66.7 mol% As_2Se_3, respectively, which is characteristic either of a non-variant equilibrium or of phase transitions of the type $\alpha \leftrightarrow \beta$. On the left and the right of these compositions the area under the thermal effects reduces which confirms the assumptions above.

We could not develop the microstructure which therefore created difficulties with regard to the measuring of HV. In order to surmount this obstacle we built the Gauss' ranges of the most probable distribution of the HV property [15]. From the characteristic appearance of these ranges the number of the phases could be judged: mono-phasic or two-phasic. The samples containing 25.0 and 66.7 mol% As_2Se_3 respectively are mono-phasic, and all the rest are two-phasic. This gives us reason to assume that intermediate compounds with compositions $3Ag_4SSe{\cdot}As_2Se_2$ and $Ag_4SSe{\cdot}2As_2Se_2$ are more likely to form with these compositions.

For the concentration ranges $0<x<25.0$; $25.0<x<66.7$ and $66.7<x<100.0$ mol% As_2Se_3 two lines are observed. The lines 1 and 4 have to be related to the starting components, Ag_4SSe and As_2Se_3 respectively, 2 and 3 – to the intermediate phases A and B – Fig. 2. The microhardness of the phases $3Ag_4SSe{\cdot}As_2Se_3$ and $Ag_4SSe{\cdot}2As_2Se_3$ is 29–31 and 41–43 kgf mm^{-2}, and that of the starting components Ag_4SSe and As_2Se_3 – 24 [16] and 70 kgf mm^{-2}, respectively [17].

The experimental results of measuring the density are shown in Fig. 3. The values obtained for d are between the values of the densities corresponding to the starting components Ag_4SSe (7.40 g cm^{-3}) [16]

Table 1 Data from indexing of phase $3Ag_4SSe{\cdot}As_2Se_3$

No.	$d_{hkl(exp)}$/Å	$100I/I_0$/%	$Q=1/d^2$	h k l	$d_{hkl(calc)}$/Å
1	4.247	8	0.0554	1 0 0	4.246
2	3.983	7	0.0630	0 1 0	3.985
3	3.824	8	0.0684	0 0 1	3.822
4	3.455	14	0.0838	$\bar{1}$ 0 1	3.453
5	3.058	35	0.1069	?	?
6	2.980	25	0.1126	1 $\bar{1}$ 0	2.978
7	2.834	100	0.1240	1 1 0	2.838
8	2.758	31	0.1315	0 1 1, 0 1 $\bar{1}$	2.758
9	2.671	12	0.1402	$\bar{1}$ 1 1	2.662
10	2.561	11	0.1525	1 1 $\bar{1}$	2.560
11	2.471	10	0.1638	1 0 1	2.470
12	2.210	11	0.2047	2 0 $\bar{1}$	2.181
13	2.159	10	0.2145	1 $\bar{1}$ 1	2.126
14	2.096	13	0.2276	1 1 1	2.073
15	2.032	14	0.2422	1 0 $\bar{2}$	2.003
16	1.989	16	0.2528	0 2 0	1.992
17	1.963	11	0.2595	$\bar{2}$ 1 1	1.954
18	1.912	11	0.2736	0 0 2	1.911
19	1.870	13	0.2860	2 1 $\bar{1}$	1.874
20	1.789	8	0.3124	1 1 $\bar{2}$	1.774
21	1.702	9	0.3452	1 2 $\bar{1}$	1.697
22	1.615	8	0.3834	$\bar{2}$ 1 2	1.607

Table 2 Data from indexing of phase $Ag_4SSe{\cdot}2As_2Se_3$

No.	$d_{hkl(exp)}$/Å	$100I/I_0$/%	$Q=1/d^2$	h k l	$d_{hkl(calc)}$./Å
1	4.330	21	0.0533	1 0 0	4.322
2	3.630	18	0.0759	0 1 0	3.631
3	3.282	22	0.0928	0 1 $\bar{1}$	3.285
4	3.210	15	0.0970	0 0 1	3.213
5	2.870	100	01214	1 0 $\bar{1}$	2.904
6	2.779	100	0.1295	1 1 0, 1 $\bar{1}$ 0	2.780
7	2.010	47	0.2475	$\bar{2}$ 0 1	2.010
8	1.988	77	0.2530	0 1 1	1.989
9	1.960	21	0.2603	1 2 $\bar{1}$	1.954
10	1.890	13	0.2799	$\bar{1}$ 1 1	1.909
11	1.800	13	0.3086	0 1 $\bar{2}$	1.816
12	1.720	21	0.3380	1 1 1	1.720
13	1.633	28	0.3750	2 0 1	1.634
14	1.440	22	0.4823	3 0 0	1.441
15	1.400	13	0.5102	1 0 2	1.408

and As_2Se_3 (4.54 g cm^{-3}) [17]. The dependency $d(x)$ is characterized with an interruption (jump) at x=25.0 and x=66.7 mol% As_2Se_3 which proves the existence of intermediate compounds with these compositions even though with narrow margins of homogeneity.

The intermediate compound $3Ag_4SSe{\cdot}As_2Se_2$ melts incongruently at 390±5°C and $Ag_4SSe{\cdot}2As_2Se_2$ congruently at 390±5°C. The two compounds endure polymorphic solid-state transition of the type $\alpha \leftrightarrow \beta$, at 105 and 120°C respectively. The liquidus lines of

Table 3 Temperatures of endothermal effects recorded on DTA curves of investigated samples

As_2Se_3/mol%	Temperature of endothermal effects/°C								
0		95							815
5	65	80						560	645
10	65	65						425	535
20	65		105				395		455
25			105				390		435
30			105				390		410
33			105			365	390		395
40			105			365			365
50			105			365			
60				120					375
67				120					390
70				120					380
75				120	330				375
80									370
90					330				360
95					330				330
100									360

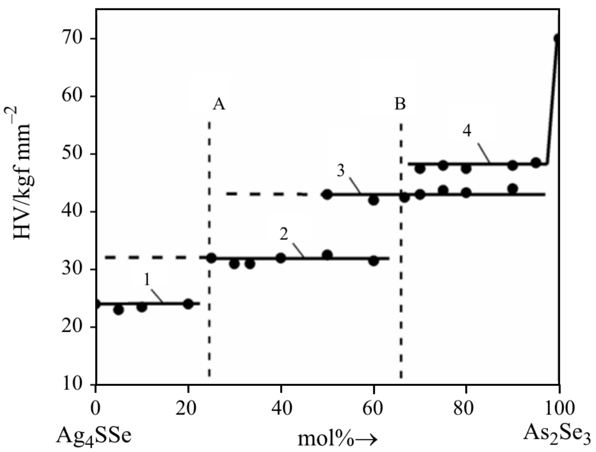

Fig. 2 Dependence HV(x) for samples of the system $Ag_4SSe–As_2Se_3$

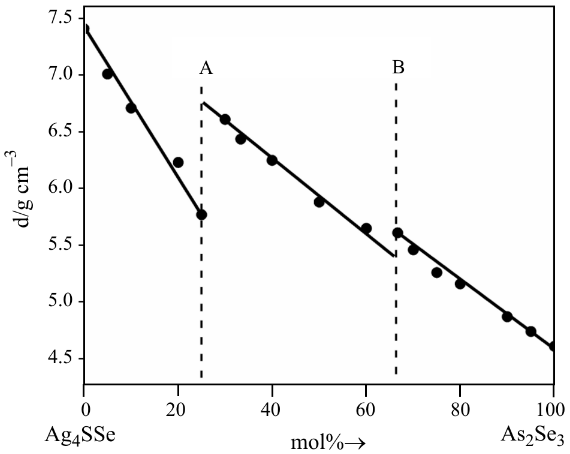

Fig. 3 Dependence $d(x)$ for samples of the system $Ag_4SSe–As_2Se_3$

the compound $Ag_4SSe{\cdot}2As_2Se_2$ form an obtuse angle, i.e. this compound tends to dissociate in a liquid-state.

The lines of two phases α-Ag_4SSe+α–*A*, α–A+α–B and α–*B*+As_2Se_3 – exist simultaneously within the concentration limits $0<x<25.0$; $25.0<x<66.7$ and $66.7<x<100$, i.e. these concentration fields correspond to three two-phase subfields of the system $Ag_4SSe–As_2Se_3$ phase diagram. The schematic diagram of the X-ray diffraction lines corresponds to the phase diagram with the formation of two intermediate compounds.

The characteristic change in the dependency HV(x) are within the concentration interval 95–100 mol% As_2Se_3 shows the presence of a homogeneity field though narrow (Fig. 2).

The dependency $d(x)$ is linear within the concentration intervals 0–25.0, 25.0–66.7 and 66.7–100.0 mol% As_2Se_3. The samples are two-phasic and refer as a mechanical mixture in which the interaction between the phases is on a physical basis.

On the basis of the data from the differential thermal analysis, the X-ray diffraction analysis and measurements of the microhardness and the density the phase diagram of the system $Ag_4SSe–As_2Se_3$ (Fig. 4) is built-up. This phase diagram is characterised with the following peculiarities:

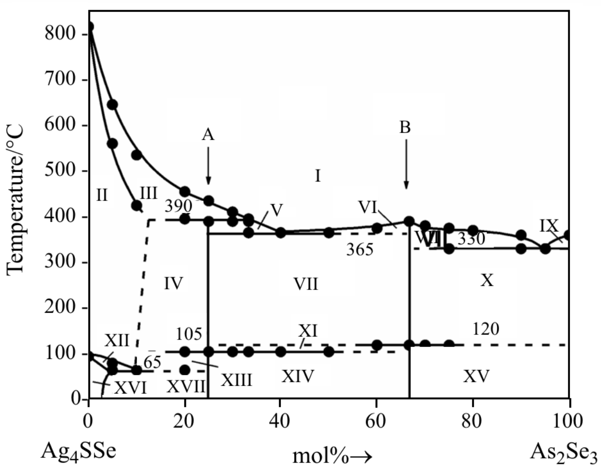

Fig. 4 Phase diagram of the system Ag_4SSe–As_2Se_3.
I – Melt-L; II – β-Ag_4SSe; III – L+β-Ag_4SSe;
IV – β-Ag_4SSe+β-$3Ag_4SSe\cdot As_2Se_3$;
V – β-$3Ag_4SSe\cdot As_2Se_3$+L; VI – L+β-$Ag_4SSe\cdot 2As_2Se_3$;
VII – β-$Ag_4SSe\cdot 2As_2Se_3$+L;
VIII – β-A-β-$Ag_4SSe\cdot 2As_2Se_3$; IX – L+As_2Se_3;
X – β-$Ag_4SSe\cdot 2As_2Se_3$+As_2Se_3;
XI – β-$3Ag_4SSe\cdot As_2Se_3$+α-$Ag_4SSe\cdot 2As_2Se_3$;
XII – α-Ag_4SSe+β-Ag_4SSe;
XIII – β-Ag_4SSe+α-$3Ag_4SSe\cdot As_2Se_3$;
XIV – α-$3Ag_4SSe\cdot As_2Se_3$+α-$Ag_4SSe_2As_2Se_3$;
XV – α-B+As_2Se_3; XVI – α-Ag_4SSe;
XVII – α-Ag_4SSe+α-$3Ag_4SSe\cdot As_2Se_3$

- There are four non-variant equilibria: one peritectic with coordinates of the peritectic point x=35 mol% As_2Se_3 and T=390°C; two eutectic at x=40 and 95 mol% As_2Se_3 and T=365 and 330°C resp. and one eutectoidal equilibrium with coordinates of the eutectoidal point x=10 mol% As_2Se_3 and T=65°C.
- As a result of various physico-chemical interactions taking place two intermediate phases with most probable compositions $3Ag_4SSe\cdot As_2Se_3$ (phase A) and $Ag_4SSe\cdot 2As_2Se_3$ (phase B). Phase A and B have polymorphic transitions respectively at 105 and 120°C, proved by the help of DTA and XRD [18–21].

The phase $3Ag_4SSe\cdot As_2Se_3$ melts incongruently, i.e. it is formed by the peritectic reaction

$$3Ag_4SSe\cdot As_2Se_3 \xrightarrow{390\pm5°C} \beta\text{-}Ag_4SSe+L$$

The peritectic point is at a composition containing around 35 mol% As_2Se_3.

The intermediate phase B melts congruently at 390±10°C but tends to dissociate (has a rounded liquidus line). It divides the phase diagram Ag_4SSe–As_2Se_3 to two sub-diagrams of eutectic type: Ag_4SSe-B and B-As_2Se_3.

- There are regions of boundary solid solutions based on Ag_4SSe. The solid solutions based on α-Ag_4SSe turn into solid solutions based on β-Ag_4SSe through the two-phase region XV of the phase diagram. The temperature of the transition α↔β depends on the composition and varies from 65 to 105°C. The regions of homogeneity based on α-Ag_4SSe expand at increasing the temperature and have maximum values at x=5 mol% As_2Se_3 and T=65°C. A shift of the As_2Se_3 lines in the concentration region 90–100 mol% is not observed at room temperature i.e. As_2Se_3 does not dissolve Ag_4SSe (the rapid change in the values of the density ΔHV=HV(100)–HV(95) proves the existence of very narrow region of homogeneity).

Conclusions

By means of four independent technics the phase diagram of the system Ag_4SSe–As_2Se_3 is built-up. As a result of complex physico-chemical processes in solid and liquid state two intermediate phases are formed with most probable compositions $3Ag_4SSe\cdot As_2Se_3$ and $Ag_4SSe\cdot 2As_2Se_3$. These two phases together with the starting components (Ag_4SSe and As_2Se_3) and the polymorphism of Ag_4SSe and the intermediate phases cause the existence of 17 phasic fields. Three of the fields are mono-phasic and the rest of them two-phasic. Of particular interest is the solid solution based on the low-temperature modification α-Ag_4SSe that possesses semiconductor properties [5, 6].

Acknowledgements

The authors acknowledge thankfully the financial support for this work from the Ministry of education and science (Fond 'Scientific investigations'-contract TN-1503/05 and 10185).

References

1 American Society of Testing Materials, Philadelphia 1969, ASTM 6-0550.
2 American Society of Testing Materials, Philadelphia 1969, ASTM 27-620.
3 J. W. Earley, Am. Mineral., 35 (1950) 337.
4 Z. Boncheva-Mladenova and K. Zaneva, J. Anorg. Allg. Chem., 437 (1977) 253.
5 V. Vassilev and Z. Boncheva-Mladenova, J. Univ. Chem. Technol. Metal. (Sofia), 27 (1984) 143 (in Bulgarian).
6 V. Vassilev and Z. G. Ivanova, Bull. Chem. Technol. Macedonia, 22 (2003) 21.
7 Z. Boncheva-Mladenova and V. S. Vassilev, Himia I Fizikohimia na poluprovodnikovite materiali, Narodna Prosveta, Sofia 1991 (in Bulgarian).
8 S. Weise and V. Kramer, J. Therm. Anal. Cal., 71 (2003) 159.
9 E. Filipec, J. Therm. Anal. Cal., 56 (1999) 1035.

10 M. Hichiri, C. Favotto, H. Zamali, Y. Feutelais, B. Legendre, A. Sebaoun and M. Jemal, J. Therm. Anal. Cal., 69 (2002) 509.
11 A. Wojakowska, E. Krzyzak and A. Wojakowski, J. Therm. Anal. Cal., 65 (2001) 491.
12 American Society of Testing Materials, Philadelphia 1969, ASTM 18–148.
13 T. Ito, X-ray studies on polymorphism, Maruzen Co. Ltd., Tokyo 1950, p. 187.
14 L. V. Vinetskii and R. A. Holodar, Statisticheskoe vzaimodeistvie elektronov i defektov v poluprovodnikov, Naukovaia Dumka, Kiev 1969 (in Russian).
15 V. Glazov and V. Virgorovich, Mikrotverdost metallov, Metallurgia, Moskva 1969 (in Russian).
16 V. S. Vassilev, V. A. Vachkov and Z. G. Ivanova, J. Mater. Sci.: In Electronics, 12 (2001) 161.
17 Z. U. Borissova, Chalkogenidnie poluprovodnikovie stekla, Leningradskogo Universiteta, Leningrad 1983 (in Russian).
18 S. A. Borkar and S. R. Dharwadkar, J. Therm. Anal. Cal., 78 (2004) 761.
19 A. Arenillas, F. Rubiera, B. Arias, J. J. Pis, J. M. Faúdez, A. L. Goldon and X. A. Garcia, J. Therm. Anal. Cal., 76 (2004) 603.
20 A. M. Abdel-Rehim, J. Therm. Anal. Cal., 76 (2004) 557.
21 M. M. Abdel-Aziz, J. Therm. Anal. Cal., 79 (2005) 709.

Received: April 20, 2005
Accepted: August 6, 2005
OnlineFirst: December 12, 2005

DOI: 10.1007/s10973-005-7063-3